AGU PUBLICATIONS

JGR

Journal of Geophysical Research: Atmospheres

RESEARCH ARTICLE
10.1002/2016JD024749

Key Points:
- At least 70% of the available energy was changed into actual evapotranspiration during wet seasons
- Soil moisture was found to be the main factor controlling energy partitioning
- The annual cumulative AET measured was 30% higher over the woodland than over the cultivated area

Correspondence to:
O. Mamadou,
ossenatou.mamadou@gmail.com

Citation:
Mamadou, O., S. Galle, J.-M. Cohard, C. Peugeot, B. Kounouhewa, R. Biron, B. Hector, and A. B. Zannou (2016), Dynamics of water vapor and energy exchanges above two contrasting Sudanian climate ecosystems in Northern Benin (West Africa), *J. Geophys. Res. Atmos.*, *121*, doi:10.1002/2016JD024749.

Received 3 JAN 2016
Accepted 5 AUG 2016
Accepted article online 10 AUG 2016

©2016. American Geophysical Union. All Rights Reserved.

Dynamics of water vapor and energy exchanges above two contrasting Sudanian climate ecosystems in Northern Benin (West Africa)

Ossénatou Mamadou[1,2], Sylvie Galle[3,4], Jean-Martial Cohard[3], Christophe Peugeot[5], Basile Kounouhewa[2], Romain Biron[3,4], Basile Hector[3], and Arnaud Bruno Zannou[6]

[1]Institut de Mathématiques et de Sciences Physiques, Porto-Novo, Bénin, [2]Laboratoire de Physique du Rayonnement, Faculté des Sciences et Techniques, Université d'Abomey–Calavi, Abomey–Calavi, Bénin, [3]LTHE, Université Grenoble Alpes, Grenoble, France, [4]LTHE, IRD, Grenoble, France, [5]HSM, IRD, Montpellier, France, [6]Ministère de l'Eau, Direction Générale des Ressources en Eau, Cotonou, Bénin

Abstract Natural ecosystems in sub-Saharan Africa are experiencing intense changes that will probably modify land surface feedbacks and consequently the regional climate. In this study, we have analyzed water vapor (Q_{LE}) and sensible heat (Q_H) fluxes over a woodland (Bellefoungou, BE) and a cultivated area (Nalohou, NA) in the Sudanian climate of Northern Benin, using 2 years (from July 2008 to June 2010) of eddy covariance measurements. The evaporative fraction (EF) response to environmental and surface variables was investigated at seasonal scale. Soil moisture was found to be the main environmental factor controlling energy partitioning. During the wet seasons, EF was rather stable with an average of 0.75 ± 0.07 over the woodland and 0.70 ± 0.025 over the cultivated area. This means that 70–75% of the available energy was changed into actual evapotranspiration during the investigated wet seasons depending on the vegetation type. The cumulative annual actual evapotranspiration (AET) varied between 730 ± 50 mm yr^{-1} at the NA site and 1040 ± 70 mm yr^{-1} at the BE site. With similar weather conditions at the two sites, the BE site showed 30% higher AET values than the NA site. The sensible heat flux Q_H at the cultivated site was always higher than that of the woodland site, but observed differences were much less than those of Q_{LE}. In a land surface conversion context, these differences are expected to impact both atmospheric dynamics and the hydrological cycle.

1. Introduction

Natural ecosystems in sub-Saharan Africa have undergone intense changes over the last few decades. Between 1975 and 2000, the area of agricultural lands increased by 57% [*Eva et al*., 2006], at the expense of forests which formerly covered 33% of the region [*Food and Agriculture Organization*, 2011; *Ouedraogo et al*., 2010]. This change was driven by high population growth [*DeFries et al*., 2010; *Guengant and Kamara*, 2012], about 2.7% per year during the 1975–2000 period [*Eva et al*., 2006; *Heldmann and Doevenspeck*, 2009], and expected to reach 4% per year by 2050 according to the most recent United Nation's projection [*UN*, 2015].

It is well known that land cover changes affect the net radiation partitioning into sensible heat and water vapor fluxes and consequently affect global atmospheric circulation [*Miralles et al*., 2011; *Numaguti*, 1993; *Pielke et al*., 2002] and the planetary boundary layer through land-atmosphere feedbacks [*Xue et al*., 2004]. These feedbacks have been identified to be particularly strong in West Africa where the surface moisture distribution drives both monsoon and squall line dynamics [*Charney*, 1975; *Koster et al*., 2004; *Taylor et al*., 2012]. Vegetation changes that impact the continental water cycle [*Amogu et al*., 2015; *Descroix et al*., 2012, 2009] are also expected to significantly affect moisture convergence, precipitation [*Wang and Eltahir*, 2000], and consequently the regional climate along with the overall hydrological cycle [*Alo and Wang*, 2010; *Weaver and Avissar*, 2001]. Therefore, studies aimed at analyzing and quantifying the water vapor and sensible heat fluxes over several ecosystems in West Africa are necessary to investigate how the observed land cover changes will impact these feedbacks under changing climatic conditions.

Several studies have focused on land surface fluxes in temperate [*Aubinet et al*., 2000; *Wilson et al*., 2002] as well as boreal climates [*Baldocchi et al*., 2004; *Baldocchi and Ryu*, 2011]. However, much less attention has been paid to the West Africa regions because of the scarcity of observations data. In this region, water vapor and energy fluxes of the Sahelian region were first analyzed after the pioneering Hapex-Sahel experiment covering a 2 months observation period [*Gash et al*., 1997]. More recently, longer periods have been analyzed

for various vegetation covers [*Brümmer et al*., 2008; *Ramier et al*., 2009; *Timouk et al*., 2009] leading to the first complete validation of land surface model simulations under Sahelian climate conditions [*Velluet et al*., 2014].

Few studies are however available for the Sudanian climate. A first study was conducted with a scintillometer over heterogeneous vegetation [*Guyot et al*., 2009]. The studied area was about 1 km^2 and included a mix of cultivated land, woodland, and a riparian forest. Although this study provided useful insights at landscape scale, no conclusions could be drawn on the contribution of the different land covers. Recently, *Mamadou et al*. [2014] analyzed water vapor and energy fluxes over 1 year (2008) above a cultivated area. This area was covered by crops alternating with herbaceous fallows [*Mamadou et al*., 2014]. The authors pointed out (i) contrasted surface responses depending on the season and (ii) the importance of surface temperature, which directly drives the longwave radiation budget and sensible heat fluxes and indirectly drives water vapor fluxes through transpiration limitations. Until now, no water vapor and sensible heat flux observations have been published for woodlands in the Sudanian region, despite their potential role in modifying land surface feedbacks to the atmosphere and their role in favoring infiltration and soil conservation.

This study is the first to compare surface exchanges over woodland and cultivated area in the Sudanian climate based over a long observation period (2 years). It analyzes the seasonal dynamics of water vapor and energy exchanges and their diurnal cycles by means of the eddy covariance (EC) technique. Both study sites are part of the AMMA-CATCH long-term observation system (www.amma-catch.org) aimed at studying the impact of climate and land surface changes on the hydrological cycle [*Lebel et al*., 2009]. In this study, we will (i) quantify the differences and identify similarities in the water vapor and energy exchanges for different land covers, (ii) identify the key factors controlling energy partitioning at the seasonal scale, (iii) evaluate the annual actual evapotranspiration (AET) and the associated uncertainties, and finally (iv) discuss the implications of land cover changes for both land surface feedbacks and the water budget under a deforestation context.

2. Materials and Methods

2.1. Study Sites

The measurements were conducted over two contrasting sites located in the Donga catchment that extends over ~600 km^2 in northern Benin, 450 km northwest of Cotonou (Figure 1). Vegetation is a patchwork of woodland (47%), shrubland (31%), and a mixture of crops and herbaceous fallow (22%) composed mainly of perennial grasses [*Seghieri et al*., 2009] (Figure 1). According to the World Reference Base (IUSS Working Group WRB, 2006), the soils are mainly ferric lixisols [*Faure and Volkoff*, 1998; *Giertz and Diekkrüger*, 2003]. The first soil horizon A (40 cm in the cultivated areas and 60 cm in the woodland) is a loamy sand with a sandy loam underneath (U.S. Department of Agriculture (USDA) soil classification). The underlying red-orcher B horizon is a sandy clay loam, the C horizon lies deeper than 1.6 m. This profile is consistent with numerous tropical soils [*de Condappa et al*., 2008]. The landscape is relatively flat overall, with gentle slope and elevation ranging between 450 and 550 m.

The two study sites are located 13 km apart in the Donga catchment. The cultivated area of Nalohou (hereafter Nalohou (NA)) is located near Nalohou village (latitude 9.74°N, longitude 1.60°E, 449 m asl). The landscape is relatively flat with local slopes not exceeding 3%. The Nalohou site is a typical cultivated area of the region, including crops and herbaceous fallow, and is dominated by C4 plants. The NA flux tower is located in a small herbaceous fallow parcel, surrounded by rotating crops (yam, maize, cassava, and groundnuts). The flux footprint is calculated with the analytical Hsieh 1-D model [*Hsieh et al*., 2000] with a 2-D extension [*Detto et al*., 2006]. It covers about 4000 m^2 during the day and more during the night, and was representative of cultivated areas of the region, including fallows (see *Mamadou et al*. [2014] for the complete footprint analysis).

The second site is located in a woodland, the most widespread vegetation type in tropical Africa [*White*, 1983], near Bellefoungou village (latitude 9.791°N, longitude 1.718°E, 445 m asl) (hereafter Bellefoungou (BE)). Vegetation of this woodland consists in an open stand of trees with crown heights of around 15 m (Figure 1b), covering 60%–80% of the total soil area [*Ago et al*., 2016]. The canopy casts little shade and an annual herbaceous layer, composed of perennial C4 vegetation which varies from 0 (dry season) to 50 cm (wet season) covers the ground. The dominant overstory species are mainly composed of C3 vegetation including: (1) *Isoberlinia tomentuosa*, (2) *Isoberlinia doka and Burkea Africana*, and (3) *Vitellaria paradoxa* [*Houéto et al*., 2012; *Seghieri et al*., 2009]. This floristic composition defines a *isoberlinia* woodland. The

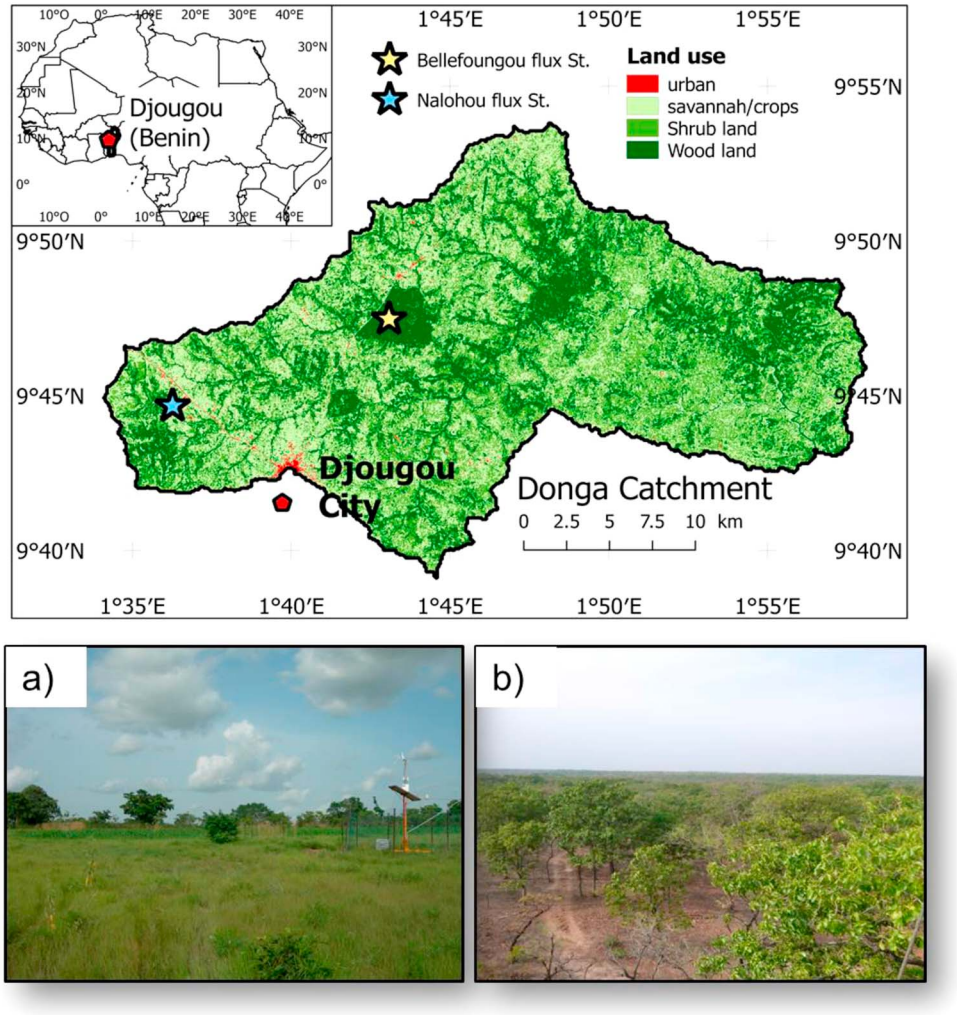

Figure 1. Locations of (a) Nalohou (cultivated area) and (b) Bellefoungou (woodland) flux stations in the Donga Catchment in Northern Benin. Shaded areas display the main land cover categories.

canopies of *Isoberlinia doka*, the dominant species at the BE site, shed at least 50% of its leaves but never 100% between November and February [*Seghieri et al*., 2012]. This species composition is reasonably homogeneous around the BE flux tower and contributes to the observed footprint (about 60,000 m^2) whatever the season [*Mamadou*, 2014]. The mean local slope is 2.5%.

The region is subjected to a Sudanian climate, driven by the fluctuation of the Intertropical Convergence Zone [*Sultan and Janicot*, 2003], is characterized by a succession of wet and dry seasons separated by two transitional periods. *Mamadou et al*. [2014] have shown that the absolute humidity (qa) can be used to delimit the seasons. The dry (qa $<6\ g\ m^{-3}$) and wet (qa $>16\ g\ m^{-3}$) seasons are separated by two transitional periods during which the absolute humidity gradually varies. The mean precipitation amount in the region is 1230 mm over the period 1950–2010. The distribution of precipitation is unimodal and more than 70% of the annual rainfall is received after the monsoon onset, between July and October [*Lelay and Galle*, 2005].

2.2. Study Period and Its Characteristics

Results presented in this paper cover two hydrological years extending from July 2008 to June 2010. The annual precipitation of the investigated years was above the mean annual rainfall: 1364 mm (2008), 1467 mm (2009), and 1534 mm (2010), respectively. According to the season definitions proposed by *Mamadou et al*. [2014], the studied periods include two "half" wet seasons (2008 and 2010), one complete wet season (2009) and two subsequent dry seasons (2008–2009 and 2009–2010). The dry seasons were short:

Table 1. Instrumentation of Nalohou (Cultivated Area) and Bellefoungou (Woodland)

Instrument	Sampling Rate	Nalohou Sensors and Manufacturers	Height (m)	Bellefoungou Sensors and Manufacturers	Height (m)
3-D sonic anemometer	20 Hz	CSAT3 Campbell Sci., USA	5	CSAT3 Campbell Sci., USA	18
Gas analyzer	20 Hz	LI-7500, Li-COR Bioscience, USA	5	LI-7500, Li-COR Bioscience, USA	18
Thermometer Hygrometerr	10 s.	WXT510, Vaisala, Finland	2	WXT510, Vaisala, Finland	5
Pyranometer	10 s.	CNR1, Kipp and Zonen, NL	2	SKS1110, Skye, NL	5
Net radiometer	10 s.	CNR1, Kipp and Zonen, NL	2	NR-Lite, Kipp and Zonen, NL	5
Raingauge	pulse	Tipping bucket ABS3030, Précis Mécanique, France	1.2	Tipping bucket ABS3030, Précis Mécanique, France	1.2
Soil thermometer	10 s.	Thermocouple 105, Campbell Sci., USA	−0.5, −0.1, −0.2, −0.4, −0.6, −1.0	Thermocouple 105, Campbell Sci., USA	−0.5, −0.1, −0.2, −0.4, −0.6, −1.0
Water content probe	10 s.	CS616, Campbell Sci., USA	−0.5, −0.1, −0.2, −0.4, −0.6, −1.0	CS616, Campbell Sci., USA	−0.5, −0.1,z −0.2, −0.4, −0.6, −1.0
Data logger		CR3000, Campbell Sci, USA		CR3000, Campbell Sci, USA	

31 and 41 days, characterized by northern Harmattan winds. The wet seasons lasted about 120 days, dominated by monsoon moisture blowing from the southwest and accompanied by heavy rainy events. Between these two seasons, drying (resp. moistening) transitional periods lasted 68 and 56 days (resp. 78 and 73 days).

2.3. Measurement Systems

Turbulent fluxes were measured continuously, from July 2008 to June 2010, using the eddy covariance (EC) system. The EC sensors (Table 1) were installed on a mast at a height of 5 m at NA and 18 m at BE, respectively.

At both sites, a complete meteorological station measuring rainfall, wind speed and direction, air temperature, relative humidity, air pressure, and a complete radiative budget was also installed (Table 1). Soil measurements included the soil moisture and the soil temperature profiles down to 1 m deep (Table 1). Meteorological data and soil measurements were recorded at a 30 min time step.

The leaf area index (LAI) at daily time step was derived from a SEVIRI satellite time series (3×3 km^2), constrained by in situ data derived from hemispherical photographs using the method proposed by *Weiss et al*. [2004].

2.4. Energy and Water Vapor Flux Computations and Data Processing

Half-hourly turbulent fluxes were computed from the covariance (equations (1) and (2)) of the vertical wind component fluctuation w' (m s^{-1}) with those of the scalar quantities, namely, air temperature T' (K) for the sensible heat flux, and absolute humidity q' (g m^{-3}) for the water vapor flux.

$$Q_H = \rho C_p \overline{w'T'}, \tag{1}$$

$$Q_{\mathrm{LE}} = \lambda \overline{w'q'}, \tag{2}$$

where ρ is the air density (kg m^{-3}), C_p the heat capacity at constant pressure (J kg^{-1} K^{-1}), and λ the latent heat of vaporization (J g^{-1}). Fluxes were computed with EdiRe software version 1.5.0.28 (University of Edinburgh, UK) using the standard procedures defined in the CarboEurope protocol [*Aubinet et al*., 2000]. Further details on data processing can be found in *Mamadou et al*. [2014]. Half-hourly Q_H and Q_{LE} data for which the quality tests [*Mauder and Foken*, 2004] were not satisfied were rejected from the data set. Eddy fluxes corresponding to the rainy events and the half-hour which followed the rainfall were also removed from the data set to avoid artifacts due to the high sensitivity of the hygrometer to raindrop extinction [*Culf et al*., 2004].

After postprocessing and filtering, 76% and 62% of Q_H and 63% and 48% of Q_{LE} at NA, and, 71% and 64% of Q_H and 64% and 40% of Q_{LE} at BE, respectively, during the 2008–2009 and 2009–2010 hydrological years, were considered suitable for further analysis.

Before filling the gaps in the data, the annual energy balance closure was evaluated for each site using the linear regression of the sum of half-hourly turbulent fluxes against the available energy (equation (3)).

$$Q_H + Q_{\mathrm{LE}} = Q - Q_G - Q_{\Delta S} \tag{3}$$

with

$$Q_{\Delta S} = S_H + S_{\mathrm{LE}} = \int_0^z \rho Cp \frac{\mathrm{d}T}{\mathrm{d}t} \mathrm{d}z + \int_0^z \lambda \frac{\mathrm{d}q}{\mathrm{d}t} \mathrm{d}z, \tag{4}$$

where Q is the net radiation and Q_G the soil heat flux estimated by the harmonic method from soil temperature and moisture profiles [*Guyot et al.*, 2009]. $Q_{\Delta S}$ is the energy storage in the air column beneath the eddy covariance system level z (m) [*Barr et al.*, 2006] and was found (not presented here) to be negligible for both sites, even at the 15 m high woodland site (less than 15 W m^{-2}). All terms in equation (3) have units of (W m^{-2}).

Ideal energy balance closure is represented by a slope of 1 and origin of zero for a plot of equation (3). For the presented data set, the average slope over the studied years was 0.84 ($r^2 = 0.92$) at NA and 0.88 ($r^2 = 0.82$) at BE. Annual values of the energy balance ratios were thus calculated as $\sum (Q_H + Q_{LE})/\sum (Q - Q_G - Q_{\Delta S})$ and were, respectively, 0.77 at NA and 0.90 at BE. These nonnegligible biases fall within the range reported for various ecosystems [*Wilson et al.*, 2002] and are classic for the EC technique [*Foken et al.*, 2011].

2.5. Statistical Analysis and Derived Quantities

2.5.1. Calculation of Midday Averages and Diurnal Cycles

Midday averages (1000–1400 UTC) of the "measured turbulent fluxes" were calculated to analyze the seasonal cycle. Indeed, more than 80% of Q_H and Q_{LE} data were available within that time slot and the dynamics were representative of the daily average values [*Mamadou*, 2014]. The evaporative fraction (EF) was also calculated using midday average fluxes.

$$EF = \frac{Q_{LE}}{Q_{LE} + Q_H}. \tag{5}$$

The diurnal cycle of energy balance components over the two sites was also characterized during the different periods of the monsoon cycle (dry and wet seasons and transitional moistening and drying periods) for the year 2009. With this objective, half-hourly data of energy balance components were averaged to build a specific composite daily cycle for each season.

2.5.2. Calculation of Bulk Parameters

The surface conductance G_s (m s^{-1}) quantifies the ability of the soil or the canopy to transfer water vapor to the atmosphere. The midday average of G_s was calculated by inversion of the Penman-Monteith equation as follows:

$$G_s = \left[\frac{1}{G_a}\left(\frac{\Delta}{\gamma}\beta - 1\right) + \frac{\rho C_p \mathrm{VPD}}{\gamma(Rn - G)}(\beta + 1)\right]^{-1}, \tag{6}$$

where Δ (Pa K^{-1}) is the slope of the saturation curve, γ (Pa K^{-1}) the psychrometric constant, VPD (Pa) the vapor pressure deficit, β the Bowen ratio, defined as Q_H/Q_{LE}, and G_a (m s^{-1}) the aerodynamic conductance, is the ability of the atmospheric surface layer to transfer water vapor from the air near the vegetation to the atmosphere, was calculated using the following equation as proposed by *Mamadou et al.* [2014]:

$$G_a = \frac{u_*}{u}\frac{\phi_H}{\phi_m}, \tag{7}$$

where u^* (m s^{-1}) is the friction velocity, u (m s^{-1}) the wind speed, and $\frac{\phi_H}{\phi_m}$ are the Businger-Dyer stability function [*Businger et al.*, 1971].

Finally, the midday average of decoupling coefficient (Ω) [*Jarvis and McNaughton*, 1986] was computed as

$$\Omega = \frac{\Delta/\gamma + 1}{\Delta/\gamma + 1 + G_a/G_s}. \tag{8}$$

(Ω) varies between 0 and 1. Values approaching zero indicate that Q_{LE} is highly sensitive to surface conductance and relative water vapor deficit, while those approaching 1 indicate that Q_{LE} is mostly controlled by net radiation [*Jarvis and McNaughton*, 1986].

For statistical analysis, the soil moisture profile was integrated to estimate the soil water content in the superficial layer (0–30 cm) and in the first meter of the soil (0–100 cm) and then normalized to be compared from one site to another. The extractable water χ was calculated as follows:

$$\chi = \left(\frac{\theta - \theta_{\min}}{\theta_{\max} - \theta_{\min}}\right), \tag{9}$$

where θ (m^3 m^{-3}) is the daily average of integrated soil moisture and $\theta_{\min}$, $\theta_{\max}$ (m^3 m^{-3}) the annual minimum and maximum of soil moisture. Finally, Spearman partial correlation between midday evaporative

fraction and its environmental and surface variables was carried out to identify the main controls of energy partitioning at seasonal scale.

2.6. Annual AET and Uncertainty Estimations

In order to estimate the annual actual evapotranspiration (AET), small gaps (i.e., < 2 h) in turbulent flux data (Q_{LE}) were filled by linear interpolation over time. Then the remaining data gaps in half-hour Q_{LE} data were filled using two approaches. Nighttime (incoming shortwave radiation lower than 10 W m^{-2}) gaps were replaced by the nighttime average seasonal values of Q_{LE}, whereas daytime gaps, if any, were filled using the linear relationships between retained values of Q_{LE} as the dependent variable and measured net radiation (Q) as the independent variable. This method assumes that EF may be considered as constant during each season. This seasonal Q_{LE}/Q fraction was relatively constant during dry and wet seasons. This was not the case during intermediate periods, but few daily values were missing during these periods. The Q_{LE} fraction of Q was determined during the different monsoon periods using linear regression with the origin forced through zero. Finally, longer gaps up to 5 days were filled using the mean diurnal variation of the variable [*Falge et al*., 2001].

The measured water vapor fluxes are affected by uncertainties due to the presence of both random (δ_{ran}) and systematic (δ_{sys}) errors. Systematic errors are difficult to estimate [*Billesbach*, 2011; *Hollinger and Richardson*, 2005]. The energy balance closure obtained ($>$0.80) in this study indicates that the systematic errors in the turbulent fluxes could be 20% if both Q_H and Q_{LE} were impacted similarly. This is intrinsic to the EC method and not considered in this study as we aim to compare two data series determined using this methodology. The remaining systematic errors were attributed to the biases due to gap filling (δ_{gap}), estimated for both daytime and nighttime fluxes. Indeed, for the nighttime fluxes, they were estimated as the standard errors of the average nighttime seasonal values of non-gap-filled Q_{LE}, whereas for the daytime fluxes, they were estimated as the standard errors of the linear regression residuals. The random error (δ_{ran}) in each half-hour flux was also estimated using the relations established by [*Richardson et al*., 2006] for grassland and forest ecosystems. The total uncertainty in the gap-filled AET, δ(AET), was finally computed at daily and annual scales by summing these three error sources as indicated in equation (10) [*Hollinger and Richardson*, 2005]. All statistical calculations (Spearman partial correlation coefficients, daily averages, and associated errors), models, and figures were made using R statistical software (R version 3.1.1).

$$\delta(\mathrm{AET}) = \sqrt{\left(\Sigma\delta^2{}_{ran} + \Sigma\delta^2{}_{gap\_nighttime} + \Sigma\delta^2{}_{gap\_daytime}\right)}. \quad (10)$$

3. Results

3.1. Meteorological and Surface Conditions

The annual cycle of incoming shortwave radiation (SW_{up}), air temperature (T_{air}), water vapor pressure deficit (VPD), soil water content (θ) at the 0–30 cm and 0–1 m layers, and leaf area index (LAI) at NA and BE are shown in Figure 2. Blue and pink shading indicate wet and dry seasons defined with the absolute humidity criteria [*Mamadou et al*., 2014].

The daily meteorological conditions of the two sites, located 13 km apart, were expectedly close except for LAI and soil moisture. At both sites, minimum annual values of SW_{up} were observed during the wet seasons mainly due to cloud cover [*Gounou et al*., 2012; *Kounouhéwa et al*., 2013]. During the dry seasons, SW_{up} was lower than its value during the moistening period (Figure 2a) due to the aerosols which are brought by the Harmattan winds in the region [*Marticorena et al*., 2010]. The VPD showed a seasonal cycle with a yearly maximum of 3 kPa and minimum of 0.8 kPa during dry and wet seasons, respectively (Figure 2c); suggesting a high atmospheric demand for water vapor fluxes. The yearly maximums of T_{air} (~30°C) were obtained during the moistening period prior to wet seasons while the minimums were observed in the wet season (Figure 2b). These daily values hide hot temperature conditions which are able to limit photosynthesis and therefore evapotranspiration as showed by *Mamadou et al*. [2014].

The seasonal variations of $\theta_{0-30\ cm}$ and $\theta_{0-1\ m}$ were consistently greater at BE than at NA (Figure 2e), but the magnitudes were similar. The increase of soil water content was earlier and faster in the woodland than on the cultivated area. This is probably due both to a lower evaporation under the shade of trees at the beginning of the season and to the roughly 10% higher rainfall observed on the woodland site during the studied years.

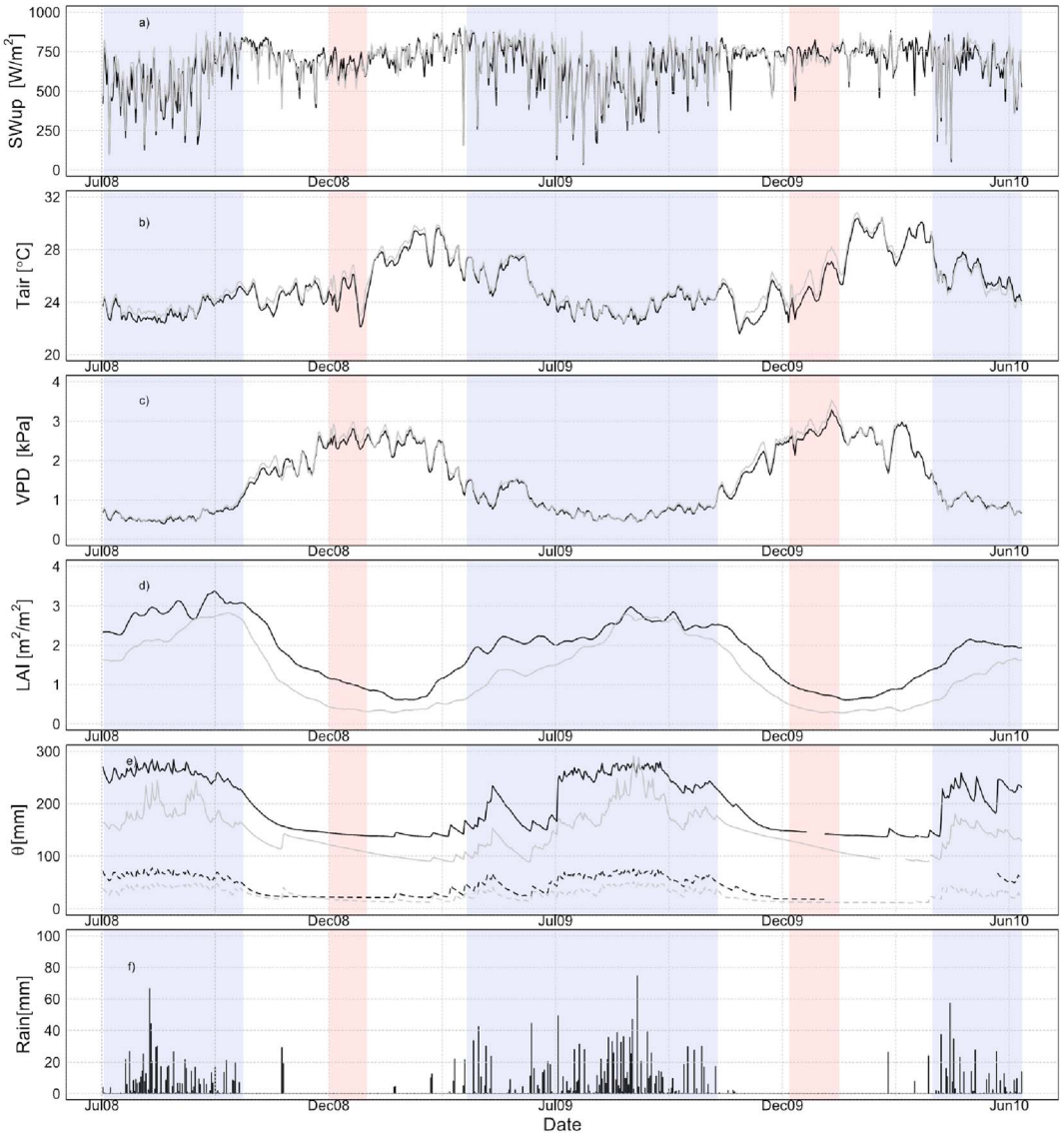

Figure 2. The 5 day average of: (a) midday incoming shortwave radiation (SW_{up}), (b) daily air temperature (T_{air}), (c) daily vapor pressure deficit (VPD), (d) daily leaf area index (LAI), (e) daily soil water content (θ) in the 0–30 cm (dotted line) and 0–1 m (solid line) layers, and (f) the daily sums of precipitation at Nalohou (gray line) and Bellefoungou (black line) during the studied years. The pink and blue shaded areas indicate, respectively, the dry and wet seasons.

The LAI of herbaceous vegetation at the NA site followed the monsoon regime (Figure 2d). The vegetated period started as soon as the first rains appeared and reached almost 3 $m^2 m^{-2}$ in the middle of the wet season, corresponding to an herbaceous height of the order of 2.5 m. Then the herbaceous fallow decayed as soon as the rains stopped. The LAI of the woodland was always higher than that of the cultivated area (Figure 2d). The woodland loses its leaves in January–February [*Seghieri et al.*, 2009] leading to a lower LAI during this period. Crop residues are burned on the cultivated site during this same period, but the LAI is nonzero due to isolated shrubs and trees in the SEVIRI pixel. Figure 2 also shows that the interannual variability in meteorological and surface variables is much greater than the intersite differences.

3.2. Dynamics of Energy and Water Vapor Fluxes

3.2.1. Midday Averages of Net Radiation

Net radiation (Q) followed a similar seasonal pattern at both sites (Figure 3a). From the beginning of the dry season, in 2009, it increased gradually from (~352 ± 28 W m^{-2} at NA and 376 ± 35 W m^{-2} at BE) to its first maximum

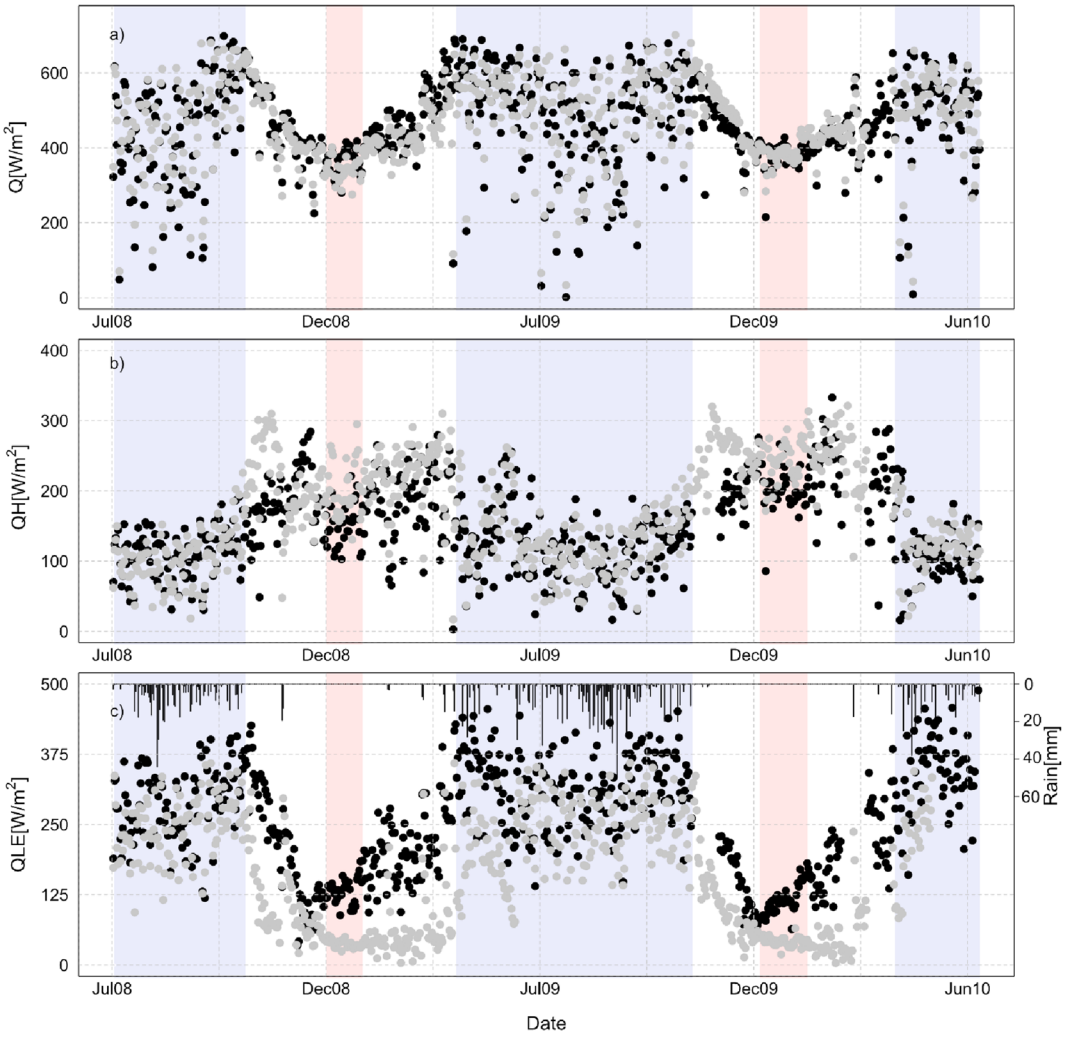

Figure 3. Midday averages of: (a) net radiation (Q), (b) sensible heat flux (Q_H), and (c) water vapor flux (Q_{LE}) at Nalohou (gray dots) and Bellefoungou (black dots) during the studied years.

at the beginning of the wet season (~580 W m^{-2}) and then decreased in the core of the wet season with a large day-to-day variability (coefficient of variation (CV): 24–30%) because of cloud cover variations [*Gounou et al.*, 2012]. The minimum values of Q observed during dry seasons were caused first by a strong increase of surface temperature which lowered the net longwave radiation and second by the presence of aerosols brought by the Harmattan winds which decreased the net shortwave radiation [*Mamadou et al.*, 2014].

3.2.2. Midday Averages of the Sensible Heat Flux

The sensible heat flux (Q_H) at both sites (Figure 3b) displayed a strong contrast between dry and wet seasons, with a high day-to-day variability during wet seasons: CV = 34% (NA) and 38% (BE). During dry seasons, high Q_H values were observed at both sites, resulting from the high surface temperature of the dry soils. Q_H at BE followed Q_H at NA closely, except after the wet season when herbaceous fallows were drying out, while the woodland canopy remained green (Figure 2d). In addition, dry vegetation was still tall (roughness length of 0.4–0.5 m) [*Mamadou*, 2014], which enhanced Q_H through greater shear. Consequently, together with high available energy (Figure 3a), this induced the highest yearly values of Q_H at the NA site (~330 W m^{-2}). At the BE site, however, the highest z_0 was observed later in the year [*Mamadou*, 2014], linked to the loss of woodland leaves [*Seghieri et al.*, 2009] that probably in turn delayed the occurrence of the yearly maximum of Q_H at this site (~290 W m^{-2}).

In response to the high soil moisture (Figure 2e) and vegetation growth (Figure 2d) during the wet season, Q_H strongly declined in association with corresponding increase in Q_{LE} (Figure 3c) but still remained

significant in the energy balance ($Q_H/Q_{LE} \sim 0.4$ at both sites). Site to site Q_H differences vanished with Q_H values comprised between 50 and 150 W m^{-2}.

3.2.3. Midday Averages of the Water Vapor Flux

The seasonal variation in water vapor flux (Q_{LE}, Figure 3c) is in phase with the associated changes in soil moisture and vegetation (Figure 2). The BE site always loses more water vapor than the NA site. Seasonal average differences between sites were about 80 and 150 W m^{-2} during wet and dry seasons, respectively (see details in section 4.1). This produced a large difference in annual Q_{LE} amounts (see further). Midday Q_{LE} values were the highest as expected during wet seasons on both sites. Although, the NA site was more sensitive than the BE site to rain breaks as observed in May 2009 when Q_{LE} dropped rapidly for the NA site only. During wet seasons, Q_{LE} displayed a high day-to-day variability driven by available energy: CV ranged between 25% and 22% at NA and BE, respectively.

During dry seasons, Q_{LE} values were nonzero at NA (~40 W m^{-2}), as already observed by *Mamadou et al.* [2014], for the year 2008. Nonzero evapotranspiration rates for cultivated areas in Sudanian climate have also been reported by *Bagayoko et al.* [2007] and farther north in the Sahel by *Gash et al.* [1997], *Ramier et al.* [2009], and *Timouk et al.* [2009]. At the BE site, Q_{LE} was 3 times higher than at the NA site (Figure 3c), despite the low values of soil moisture. Moreover, soil moisture ($\theta_{0-1\,m}$) decreased less at the BE site than at NA site (Figure 2e). This suggests that the transpiration activity of woodland in this season was supplied by deeper soil layers (below 1 m depth).

During the moistening period, the difference in evapotranspiration amounts between the two ecosystems was maximum. While Q_{LE} started to increase at the end of the dry season at the BE site, it remained low and was subjected to isolated rainy events at the NA site. The growth of Q_{LE} at NA follows more or less the LAI dynamics which started to increase toward the end of the moistening period. Finally, during the drying period, the decrease of Q_{LE} at the BE site was also delayed compared to the decrease at the NA site. Woodlands evapotranspiration seems to be less sensitive to the lack of rain than the cultivated area.

3.2.4. Diurnal Cycles of Exchanges Between Two Ecosystems and the Atmosphere

Figures 4a–4d show seasonal averages of the composite diurnal cycles of net radiation (Q), sensible heat (Q_H), and water vapor fluxes (Q_{LE}) for both sites. The diurnal cycle of Q at the BE site displays a slight hollow during morning hours caused by branch's shading , especially during the drying period because the measured net radiation at that site corresponded to the understory net radiation. We again observed higher Q_{LE} at BE than at NA, whatever the season, excepted during night-day and day-night transitions when Q_{LE} have the same order of magnitude considering measurement uncertainties during these transitions. In the afternoon, Q_H at NA lasted more than at BE in all seasons. This could be associated with the sustained Q_{LE} at BE, which probably limits surface temperature through latent heat processes. We finally observed that Q_{LE} often met and/or exceeded Q from the afternoon to the evening and remained positive during nighttime, indicating water vapor losses at both sites. Nocturnal evapotranspiration has already been observed at the cultivated site [*Mamadou et al.*, 2014], thus suggesting nocturnal evaporation or an incomplete stomata closure [*Caird et al.*, 2007; *Snyder*, 2003]. These findings corroborated those obtained by *Novick et al.* [2009] which showed that nocturnal evapotranspiration across a wide range of species in Southeastern US averaged 8–9% of mean daytime evapotranspiration and *Awessou et al.* [2016] that evidenced nocturnal transpiration on *Vitellaria paradoxa* trees of the Bellefoungou woodland. On the other hand, nighttime Q_H was negative in all seasons, meaning that sensible heat was lost from the ecosystem to the atmosphere. This, together with ground heat release, participated in balancing the surface energy loss through longwave radiative emissions, thus allowing ongoing evapotranspiration (Figures 4a–4d).

For the dry season, Q_H was the main consumer in the energy balance and reached a maximum value of 215 $\pm$ 46 W m^{-2} at NA and 183 $\pm$ 44 W m^{-2} at BE, at midday. Q_H at BE was slightly delayed compared with the dynamics of Q_H at NA, which was not the case for Q_{LE} that responded to sunrise at both sites. The maximum values of Q_{LE} at BE occurred in the morning during this season. As soil moisture changed very little from morning to afternoon (less than 0.1 mm) during the dry season, this is probably caused by a temperature limitation of stomatal opening.

During the wet season (Figure 4b), Q_{LE} became the main consumer of the available energy at both sites. Q_H cycles were very close despite the vegetation differences. A phase shift of about 1 h can be clearly observed

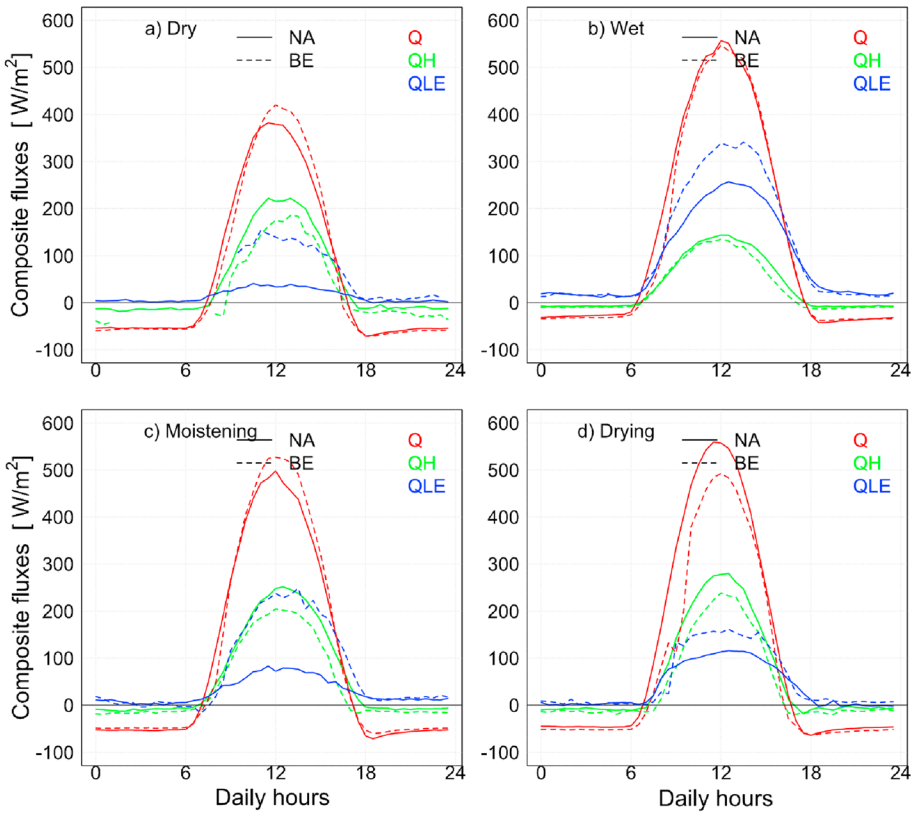

Figure 4. Composite diurnal cycles of energy balance components for the different monsoon periods of the year 2009: (a) dry and (b) wet seasons and (c) moistening and (d) drying periods in the woodland (dotted line) and cultivated (solid line) sites. The net radiation (Q), sensible heat (Q_H), and water vapor (Q_{LE}) fluxes are plotted, respectively, in red, green, black, and blue colors.

between Q_H and Q_{LE} at both sites. Q_H followed the dynamics of Q more closely than the dynamics of Q_{LE}, which were delayed in the afternoon.

During the drying period, the soil and the atmosphere become drier. Q_H became the main consumer of the available energy at both sites with a typical bell-shaped diurnal cycle in phase with that of Q (Figure 4d), whereas Q_{LE} was flattened at midday at both sites. The latter is probably associated with the senescence of the vegetation, which becomes less efficient [*Gee and Federer*, 1972; *Seghieri et al.*, 2009].

3.3. Energy Partitioning and Its Controlling Factors

3.3.1. Environmental and Surface Controls

The evaporative fraction (EF) clearly shows a seasonal cycle at both sites, with some interannual variations that are more distinct in the dry and transitional seasons (Figure 5). It remained rather stable during the wet seasons, especially in the core of the wet season when median EF values equaled 70 ± 2.5% at NA and 75 ± 0.7% at BE, respectively. This means that 70–75% of the available energy was changed into actual evapotranspiration during the wet season.

The effect of soil water content variations on energy partitioning was further examined via the relationship between EF and the extractable water χ (Figures 6a and 6b). A significant positive relationship (Spearman partial correlation $r = 0.41$ (NA); $r = 0.36$ (BE); and $p < 0.0001$) was found between EF and $\chi_{0-30\,cm}$ at both sites (Table 2). EF increased with surface soil water content until a threshold of 50% at NA and 20% at BE, above which $\chi_{0-30\,cm}$ no longer influenced EF (Figure 6a).

The relationship with the deeper soil layer (30 cm–100 cm) (Figure 6b) is less clear as illustrated by the Spearman partial correlations (Table 2) which are negative at both sites: $r = -0.28$ (NA) and $r = -0.26$ (BE).

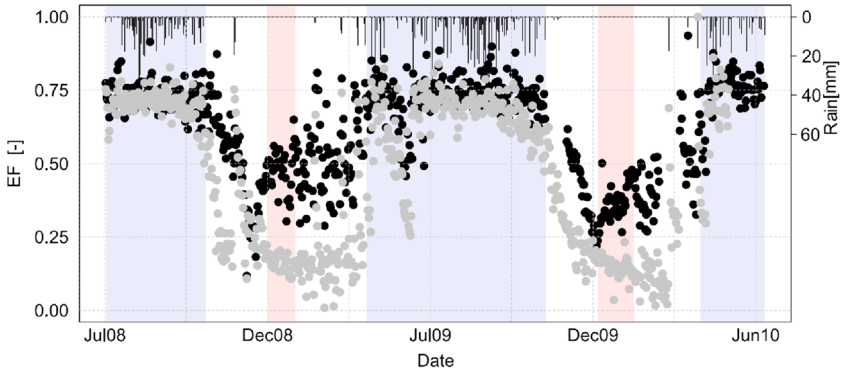

Figure 5. Midday evaporative fraction (EF) at Nalohou (gray dots) and Bellefoungou (black dots) during the studied years.

However, as the extractable water contents in the 0–30 cm and 30–100 cm soil layers are intercorrelated ($r = 0.63$; $r = 0.46$; and $p < 0.0001$), it is not possible to separate their respective influences on EF.

During the wet season, VPD was below 1.7 kPa, (Figure 2c) and seemed to have no visible influence on EF variations at either site (Figure 6c). For high VPD values (>3 kPa), EF also remained more or less stable but with a different level for NA (EF = 20%) and BE (EF = 45%). Between these two VPD values (1.7 kPa < VPD < 3 kPa), both ecosystems show a linear VPD dependency. The decreasing linear gradient obtained was higher at the NA site ($-0.38\ kPa^{-1}$) than at the BE site ($-0.23\ kPa^{-1}$). This likely reflects the sensitivity of AET to VPD during intermediate periods. Both sites show a sensitivity of EF to soil moisture, VPD, and LAI. These variables are intercorrelated. The seasonal contrast drives the energy partitioning and the dynamics of all the parameters.

3.3.2. Aerodynamic Conductance, Surface Conductance, and Decoupling Coefficient

The aerodynamic conductance (G_a) was nearly constant at NA (~100 mm s^{-1}), while it showed a strong seasonal variability at BE (Figure 7a). The BE lowest values (150 mm s^{-1}) were observed during the wet season; during the other seasons, the observed values were systematically higher and reached 250 mm s^{-1} in the 2010 dry season. These highest values correspond to the renewing of leaves and a subsequent higher

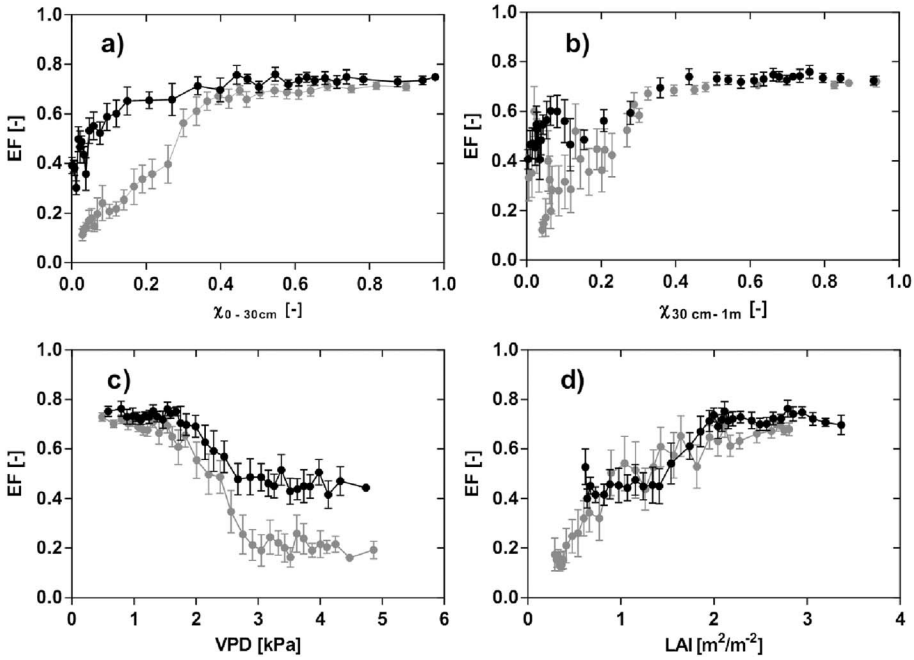

Figure 6. Relationship between midday evaporative fraction (EF) versus: (a) extractable soil water between 0 and 30 cm, (b) extractable soil water between 30 cm and 1 m, (c) the water vapor deficit (VPD), and (d) leaf area index at Nalohou (gray colors) and Bellefoungou (black colors) during the studied years. Each point on the graph is a bin average over 20 measurements. The error bars represent the 95% confidence interval.

Table 2. Spearman Partial Correlations Calculated for the Two Studied Years Showing Relations Between Evaporative Fraction (EF) and Some Physical Predictor Variables[a]

CULTURE	EF	VPD	T_{air}	$\chi_{0-30\,cm}$	$\chi_{30\,cm-1\,m}$	LAI
EF	1					
VPD	−0.21(***)	1				
T_{air}	−0.11(**)	0.65(***)	1			
$\chi_{0-30\,cm}$	0.41(***)	−0.17(***)	−0.08(*)	1		
$\chi_{30\,cm-1\,m}$	−0.28(***)	0.26(***)	−0.20(***)	0.46(***)	1	
LAI	0.23(***)	−0.36(***)	0.26(***)	0.19(***)	0.48(***)	1

WOODLAND	EF	VPD	T_{air}	$\chi_{0-30\,cm}$	$\chi_{30\,cm-1\,m}$	LAI
EF	1					
VPD	−0.13(**)	1				
T_{air}	−0.01(NS)	0.71(***)	1			
$\chi_{0-30\,cm}$	0.36(***)	−0.54(***)	0.34(***)	1		
$\chi_{30\,cm-1\,m}$	−0.26(***)	0.30(***)	−0.41(***)	0.63(***)	1	
LAI	0.22(***)	−0.18(***)	0.17(***)	−0.08(NS)	0.62(***)	1

[a]Predictor variables: water vapor deficit (VPD), air temperature (T_{air}), extractable soil water in the 0–30 cm layer ($\chi_{0-30\,cm}$) and 30 cm–1 m layer ($\chi_{30\,cm-1\,m}$) at Nalohou (culture) and Bellefoungou (woodland). The partial correlation (r) and significance level are indicated for each regression; nonsignificant NS ($p > 0.05$). *weakly significant for $p < 0.01$. **moderately significant for $p < 0.001$. ***highly significant for $p < 0.0001$.

roughness length. The highest surface conductance (G_s) was observed during the wet season (Figure 7b) with mean seasonal maxima values of $11.1 \pm 0.6\,mm\,s^{-1}$ (NA) and $12 \pm 0.5\,mm\,s^{-1}$ (BE). Figures 7a and 7b also show that the values of G_a ($100–250\,mm\,s^{-1}$) are far greater than those of G_s ($<20\,mm\,s^{-1}$), suggesting that the sensitivity of G_s to G_a is low as demonstrated by *Granier et al.* [1996]. The aerodynamic resistance ($1/G_a$) contribution was indeed always less than 1% of the surface resistance ($1/G_s$).

The decoupling coefficient (Ω) (Figure 7c) showed seasonal changes similar to those of G_s. In the two ecosystems, Ω seasonal averages ranged from 0.05 to 0.45, during the dry and wet seasons respectively. However, in the wet seasons, seasonal maxima values of Ω obtained were slightly lower at BE than at NA, probably because of a higher roughness length at the woodland site ($z_0 \sim 1.2$ m) than at the cultivated site ($z_0 \sim 0.45$ m at the end of the wet season) which favored more surface atmosphere coupling through a mixing of the air within the canopy and atmosphere at the woodland site.

3.4. Annual Actual Evapotranspiration (AET)

The annual sums of AET for the two studied years are shown in Table 3. For both sites, the measured total annual evapotranspiration varied little over the two studied years. The 12% (resp.15%) increase of annual rainfall from the 2008–2009 to the 2009–2010 year observed at NA (resp. BE) does not seem to have induced

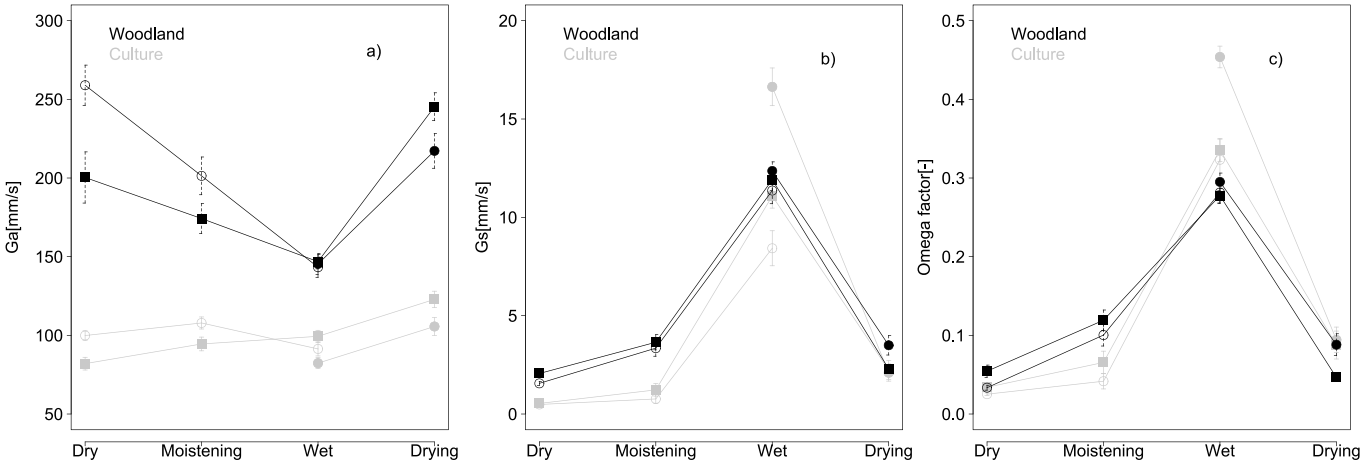

Figure 7. Seasonal means values of: (a) aerodynamic conductance (G_a), (b) surface conductance (G_s), and (c) decoupling coefficient factor (Ω) at Nalohou (gray) and Bellefoungou (black) during the years 2008 (solid circles), 2009 (squares), and 2010 (empty circles). The error bars represent the 95% confidence interval.

Table 3. Seasonal and Interannual Sums of Precipitation (P), Actual Evapotranspiration (AET), Percent of Precipitation That Returns Into the Atmosphere Through Evapotranspiration (AET/P) Over the Woodland and Cultivated Area During the Two Hydrological Years 2008–2009 and 2009–2010

					Bellefoungou (Woodland)			Nalohou (Culture)		
Years	Seasons	Beginning	End	Length (days)	P (mm)	AET (mm ± SE)	AET/P(%)	P (mm)	AET (mm ± SE)	AET/P(%)
2008/2009	Wet	01/07/08	19/10/08	111	880	342 ± 33	39	797	318 ± 21	40
	Drying	20/10/08	26/12/08	68	1	167 ± 16	>100	55	93 ± 10	>100
	Dry	27/12/08	26/01/09	31	0	46 ± 28	>100	0	15 ± 2.4	>100
	Moistening	27/01/09	14/04/09	78	120	203 ± 31	>100	74	75.5 ± 18	>100
	Wet	15/04/09	30/06/09	78	355	289 ± 26	81	289	219 ± 16	76
	Year 1	01/07/08	30/06/09	366	1356	1047 ± 62	77	1215	721 ± 34	59
2009/2010	Wet	01/07/09	31/10/09	123	1119	428 ± 33	38	930	372 ± 27	40
	Drying	01/11/09	26/12/09	56	30	99 ± 35	>100	20	71 ± 25	>100
	Dry	27/12/09	05/02/10	41	0	57 ± 17	>100	0	22.5 ± 3	>100
	Moistening	06/02/10	19/04/10	73	40	178 ± 42	>100	53	71 ± 23	>100
	Wet	20/04/10	30/06/10	73	367	272 ± 45	74	354	199 ± 46	56
	Year 2	01/07/09	30/06/10	366	1557	1034 ± 80	66	1356	736 ± 63	54

a concomitant increase in annual AET (<2%; Table 3). On the other hand, the average annual sum of AET at the woodland site (1040 ± 70 mm) was 30% higher than that of the cultivated area (730 ± 50 mm). The ratio of annual AET to annual rainfall was 72% and 57%, respectively, at the woodland and cultivated sites. In the cultivated area, 76% of the annual AET occurs during the wet season (554 ± 55 mm), while this percentage is only 64% over the woodland (665 ± 68 mm). The AET amount is distributed more evenly over the year on the woodland site than on the cultivated area.

4. Discussion

4.1. Ecosystem Differences

Our study indicates that the two ecosystems responded to meteorological (and soil moisture) variations during the dry and intermediate seasons. They were less sensitive to these variables in the wet season but remained mainly driven by the available energy. The intersite differences in the surface energy and water vapor exchanges were much greater than the interannual differences for these two wet years. Both sites had similar meteorological forcing and soil properties; thus, observed surface exchange differences were mainly due to difference in ecophysiological properties.

4.1.1. Wet Seasons

During the wet seasons, the thermal gradient of the surface boundary layer was almost equal [*Lohou et al*., 2010] in both ecosystems and their exchanges in terms of sensible heat flux were similar (absolute difference lower than 20 W m^{-2}). The difference in Q_{LE} was greater as Q_{LE} varied on the average between 240 W m^{-2} (NA) and 320 W m^{-2} (BE). However, the absolute difference in their evaporative fraction was about 5% (Figure 5). Overall, average values of EF during the wet seasons obtained at BE (0.75) were comparable with reports of 0.73–0.75 obtained over a savanna region in Burkina-Faso [*Bagayoko et al*., 2007; *Brümmer et al*., 2008]. At the NA site, EF (0.70) was slightly higher than the 0.67 values reported by [*Guyot et al*., 2012] from scintillometry measurements over a region with heterogeneous vegetation in northern Benin.

4.1.2. Dry Seasons

During the dry seasons, no rain occurred and the available soil moisture was different for the two vegetation covers, depending on their root system depth. In the cultivated area, the crops grow new roots each year within the first meter of the soil, while the roots of trees in the woodland continue to grow and can reach deeper soil over the years. This factor led to both higher actual evapotranspiration (Figure 3c) and transpiration rates (G_s ~ 3 mm/s; Figure 7b) at the woodland site. Similar results were found by *Juárez et al*. [2007] and *Vourlitis et al*. [2002] over the Amazonian forest where the dry season lasts more than 4 months without any rainfall. These high transpiration rates are due to vegetation activity which even leads to leaf renewal during this dry season in the region [*Seghieri et al*., 2009]. It is also associated with high physiological activity as shown in the sap flow analysis [*Awessou et al*., 2016] as well as in the CO_2 fluxes [*Ago et al*., 2016, 2015, 2014] in the studied area. This phenomenon was also observed farther north above a savanna in Ghana by *Quansah et al*. [2015].

4.1.3. Comparison With Other Tropical Ecosystems

The role of deep roots in the transpiration process, especially above forests, has been pointed out in other climatic contexts [*Collins and Bras*, 2007; *Feddes et al*., 2001; *Nepstad et al*., 1994]. In the Sudanian climate, the soil moisture in the 0–1 m layer was low and did not vary too much during dry seasons (Figure 2e), which indicates that the trees extract water from deeper soil layers. Since the maximum rooting depth is about 15 ± 5.4 m for tropical grassland/savanna [*Canadell et al*., 1996], this probably favors the extraction of water from deep layers, since a depletion of permanent groundwater was already observed during the dry season in the region [*Séguis et al*., 2011; *Vouillamoz et al*., 2015]. The ability of trees to extract available water from deep soil layers allows them to survive in the dry season. Consequently, the major differences in AET between the two ecosystems are observed during the moistening and the drying periods (Table 3).

On the average, annual actual evapotranspiration represents 57% of the rainfall at the cultivated site and 72% at the woodland site (Table 3). These percentages are in the same range but slightly higher than those obtained over Sahelian sites (Niger—Lat: 13.65°N-600 mm yr^{-1} of rain). Using the eddy covariance technique, *Ramier et al*. [2009] found, on the average for a two years period, that AET was 65% (resp. 45%) of the annual rain amount for a fallow (resp. a millet crop) site. In another tropical region, a 7 year average of 52% was found by *Vourlitis et al*. [2015], using the eddy covariance technique above a semideciduous forest in the rainforest-savanna of northern Mato Grosso, Brazil. All these observations are probably a lower bound for the total amount of AET because of underestimation of turbulent fluxes associated with the eddy-covariance technique [*Foken et al*., 2011]. This underestimation was already pointed out by *Velluet et al*. [2014] whose simulations showed a 4 year AET average of 82–85% of the total amount of rain for the Niger rain-fed millet crop and fallow bush, whereas *Ramier et al*. [2009] measured 45%–65% over the same sites. However, differences between sites subjected to the same atmospheric forcing can obviously be compared and analyzed in terms of land cover change. The difference of ~300 mm between the two sites is probably a reliable order of magnitude.

4.2. Implication for Land Surface Feedbacks and Water Balance

The lower albedo and surface temperature of woodlands [*Bonan*, 2008] increases net radiation, thereby favoring water vapor flux losses in the energy budget partition (Figure 3c). The conversion of woodland into cultivated areas would thus probably induce some changes in land surface feedbacks, returning less water vapor to the atmosphere (Table 3) and therefore less latent heat energy. At the same time, on an annual basis, cumulative sensible heat fluxes are close from one site to another. Therefore, in terms of energy transfer, these observations suggest that land conversion from woodland to cultivated areas in this Sudanian region would probably not participate greatly to the heating of the atmosphere through sensible heat fluxes but would reduce the latent (and hence the water vapor) fluxes to the atmosphere, specifically during the moistening period (Figure 3c). This atmosphere moistening process has been identified [*Lothon et al*., 2008] as a major contributing factor in the onset of the rainy season. A reduction in the moistening of the atmosphere by the surface should therefore impact the onset of the rainy season and probably the monsoon dynamics over the region [*Koster et al*., 2004].

Land conversion from woodlands to cropping areas should also affect the hydrologic cycle, especially the groundwater dynamics. For instance, land clearing would be expected to produce a rise in the groundwater level as deep water uptake is reduced. Such processes have been reported in other regions [*Kelly et al*., 2016; *Krishnaswamy et al*., 2012; *Moore et al*., 2012; *Peña-Arancibia et al*., 2012; *Zhang et al*., 2012]. However, despite drastic deforestation since in Benin 1973 (from 70% to 25% of the total surface), the upper Oueme river discharge (a 15,000 km^2 catchment in which the Donga catchment is embedded) has not shown any great change [*Lelay and Galle*, 2005; *Peugeot et al*., 2011]. As shown by *Hector et al*. [2015] and *Séguis et al*. [2011], river flows over recent years in this area mainly originate from perched, seasonal water tables and the contribution of deep (10–20 m) groundwater is negligible. At the hillslope scale, *Richard et al*. [2013] conducted a virtual experiment that showed that the riparian forest plays a major role in disconnecting the water table from the river flow. Annual aquifer recharge in northern Benin has been quantified to be between 100 and 400 mm depending on the ground lithology [*Vouillamoz et al*., 2015]. The AET decrease due to deforestation lies within this range and we have shown that it is partially drawn from deep ground layers. These first AET observations in northern Benin therefore gave rise to many questions concerning the water budget: How aquifer recharge would be impacted by land cover changes? Would ground storage capacity be sufficient to store the excess of the water budget? What is the effect of rainfall variability and land cover changes on river discharges and water table level? To answer such questions, longer series of water budget observations will

be required along with hydrological models that can simulate vertical and horizontal water transfers from rain to the water table and rivers, taking into account surface and vegetation processes. Changes in the continental hydrological cycle could also in turn impact feedbacks to the atmosphere related to increased accessible water close to the surface. Once again, models including both the continental and atmospheric hydrological cycle could help us to answer such questions [*Maxwell et al*., 2010].

5. Conclusion

This study, using 2 years of eddy covariance data, is the first to compare the dynamics of water vapor and sensible heat fluxes of a woodland and a cultivated area in Sudanian West Africa. To our knowledge, it represents the longest continuous field scale data set of turbulent fluxes of these ecosystems published so far for the Sudanian climate. At seasonal scale, we have shown that soil moisture is the main controlling factor of the net radiation partitioning into sensible and water vapor fluxes. The seasonality of the sensible heat flux has been clearly demonstrated for both sites. Depending on the season, the seasonal cumulative water vapor loss of the woodland differed from that of the cultivated area by a factor of 1.2 (wet season) up to 3 (dry season). Globally, the AET amount is distributed more evenly over the year on the woodland site than on the cultivated area. The average annual AET measured during the investigated years represented 57% and 72% of the annual rainfall over the cultivated area and the woodland, respectively. The differences in the water vapor fluxes of the two ecosystems (30%) were much higher than the interannual variability (<2%). They could impact the hydrological cycle, but the available time series are not long enough to draw firm conclusions. Moreover, the studied years were characterized by wet atmospheric conditions compared to the 50 year local mean precipitation. For this reason, we have not been able to clarify the effects of woodland and cultivated land cover under water stress conditions. More years of measurements including dry weather conditions are thus necessary to consolidate these findings.

Acknowledgments

The first author received a scholarship from the "Institut de Recherche pour le Développement (IRD)," "Agence Universitaire pour la Francophonie (AUF, Bureau Afrique de l'Ouest)," and "Université d'Abomey-Calavi (UAC, Bénin)." This work was supported by grants from "Ouémé2025" (Fond de Solidarité Prioritaire FSP/RIPIECSA), Labex OSUG@2020 (Investissements d'avenir—ANR10 LABX56), the "International Foundation of Science," project Water N°5422-1 and from the "Intergovernmental Panel on Climate Change (IPCC)." The AMMA-CATCH regional observation system (http://www.amma-catch.org) was set up thanks to an incentive funding of the French Ministry of Research that allowed the pooling of various preexisting small-scale observation setups. The short and long term continuity of the measurements is made possible by undisrupted IRD funding since 1990 and by continuous CNRS-INSU funding since 2005, in cooperation with the "Direction Générale de l'Eau (DG-Eau)" in Bénin. The authors are grateful to the staff of AMMA-CATCH Benin: Simon Afouda, Simon Alloganvinon, Stéphane Boubkraoui, Théo Ouani, Alexandro Pixano, Jules Sogba-Goh, and Maxime Wubda for their permanent support for data collection in the field. We thank Harvey Harder for reviewing and improving the English of our manuscript. The authors declare that there is no conflict of interest regarding the publication of this paper.

References

Ago, E. E., E. K. Agbossou, S. Galle, J.-M. Cohard, B. Heinesch, and M. Aubinet (2014), Long term observations of carbon dioxide exchange over cultivated savanna under a Sudanian climate in Benin (West Africa), *Agric. For. Meteorol.*, *197*, 13–25, doi:10.1016/j.agrformet.2014.06.005.

Ago, E. E., D. Serça, E. K. Agbossou, S. Galle, and M. Aubinet (2015), Carbon dioxide fluxes from a degraded woodland in West Africa and their responses to main environmental factors, *Carbon Bal. Manag*, 10, doi:10.1186/s13021-015-0033-6.

Ago, E. E., E. K. Agbossou, J.-M. Cohard, S. Galle, and M. Aubinet (2016), Response of CO_2 fluxes and productivity to water availability in two contrasting ecosystems in northern Benin (West Africa), *Ann. For. Sci.*, doi:10.1007/s13595-016-0542-9.

Alo, C. A., and G. Wang (2010), Role of dynamic vegetation in regional climate predictions over western Africa, *Clim. Dyn.*, *35*, 907–922, doi:10.1007/s00382-010-0744-z.

Amogu, O., et al. (2015), Runoff evolution due to land-use change in a small Sahelian catchment, *Hydrol. Sci. J.*, *60*, 78–95, doi:10.1080/02626667.2014.885654.

Aubinet, M., et al. (2000), Estimates of the annual net carbon and water exchange of forests: The EUROFLUX methodology, *Adv. Ecol. Res.*, *30*, 113–175.

Awessou, K. G. B., C. Peugeot, A. Rocheteau, L. Seguis, F. C. Do, S. Galle, M. Bellanger, E. Agbossou, and J. Seghieri (2016), Differences in transpiration between a forest and an agroforestry tree species in the Sudanian belt, *Agrofor. Syst.*, doi:10.1007/s10457-016-9937-8.

Bagayoko, F., S. Yonkeu, J. Elbers, and N. van de Giesen (2007), Energy partitioning over the West African savanna: Multi-year evaporation and surface conductance measurements in Eastern Burkina Faso, *J. Hydrol.*, *334*, 545–559.

Baldocchi, D. D., and Y. Ryu (2011), A synthesis of forest evaporation fluxes—from days to years—as measured with eddy covariance, in *Forest Hydrology and Biogeochemistry*, edited by D. F. Levia, D. Carlyle-Moses, and T. Tanaka, pp. 101–116 , Ecological Studies, Springer Netherlands.

Baldocchi, D. D., L. Xu, and N. Kiang (2004), How plant functional-type, weather, seasonal drought, and soil physical properties alter water and energy fluxes of an oak–grass savanna and an annual grassland, *Agric. For. Meteorol.*, *123*, 13–39.

Barr, A. G., K. Morgenstern, T. A. Black, J. H. McCaughey, and Z. Nesic (2006), Surface energy balance closure by the eddy-covariance method above three boreal forest stands and implications for the measurement of the CO_2 flux, *Agric. For. Meteorol.*, *140*, 322–337, doi:10.1016/j.agrformet.2006.08.007.

Billesbach, D. P. (2011), Estimating uncertainties in individual eddy covariance flux measurements: A comparison of methods and a proposed new method, *Agric. For. Meteorol.*, *151*, 394–405, doi:10.1016/j.agrformet.2010.12.001.

Bonan, G. B. (2008), Forests and climate change: forcings, feedbacks, and the climate benefits of forests, *Science*, *320*, 1444–1449, doi:10.1126/science.1155121.

Brümmer, C., U. Falk, H. Papen, J. Szarzynski, R. Wassmann, and N. Brüggemann (2008), Diurnal, seasonal, and interannual variation in carbon dioxide and energy exchange in shrub savanna in Burkina Faso (West Africa), *J. Geophys. Res.*, *113*, G02030, doi:10.1029/2007JG000583.

Businger, J. A., J. C. Wyngaard, Y. Izumi, and E. F. Bradley (1971), Flux-profile relationships in the atmospheric surface layer, *J. Atmos. Sci.*, *28*, 181–189, doi:10.1175/1520-0469(1971)028<0181:FPRITA>2.0.CO;2.

Caird, M. A., J. H. Richards, and L. A. Donovan (2007), Nighttime stomatal conductance and transpiration in C3 and C4 plants, *Plant Physiol.*, *143*, 4–10, doi:10.1104/pp.106.092940.

Canadell, J., R. B. Jackson, J. B. Ehleringer, H. A. Mooney, O. E. Sala, and E.-D. Schulze (1996), Maximum rooting depth of vegetation types at the global scale, *Oecologia*, *108*, 583–595, doi:10.1007/BF00329030.

Charney, J. G. (1975), Dynamics of deserts and drought in the Sahel, *Q. J. R. Meteorol. Soc.*, *101*, 193–202, doi:10.1002/qj.49710142802.

Collins, D. B. G., and R. L. Bras (2007), Plant rooting strategies in water-limited ecosystems, *Water Resour. Res.*, *43*, W06407, doi:10.1029/2006WR005541.
Culf, A. D., T. Foken, and J. H. C. Gash (2004), The energy balance closure problem, In *Vegetation, Water, Humans and the Climate. A New Perspective on an Interactive System*, P. Kabat et al., pp. 159–166, Springer-Verlag, Heidelberg.
de Condappa, D., S. Galle, B. Dewandel, and R. Haverkamp (2008), Bimodal zone of the soil textural triangle: Common in tropical and subtropical regions, *Soil Sci. Soc. Am. J.*, *72*, 33, doi:10.2136/sssaj2006.0343.
DeFries, R. S., T. Rudel, M. Uriarte, and M. Hansen (2010), Deforestation driven by urban population growth and agricultural trade in the twenty-first century, *Nat. Geosci.*, *3*, 178–181, doi:10.1038/ngeo756.
Descroix, L., et al. (2009), Spatio-temporal variability of hydrological regimes around the boundaries between Sahelian and Sudanian areas of West Africa: A synthesis, *J. Hydrol.*, *375*, 90–102, doi:10.1016/j.jhydrol.2008.12.012.
Descroix, L., P. Genthon, O. Amogu, J.-L. Rajot, D. Sighomnou, and M. Vauclin (2012), Change in Sahelian Rivers hydrograph: The case of recent red floods of the Niger River in the Niamey region, *Global Planet. Change*, *98-99*, 18–30, doi:10.1016/j.gloplacha.2012.07.009.
Detto, M., N. Montaldo, J. D. Albertson, M. Mancini, and G. Katul (2006), Soil moisture and vegetation controls on evapotranspiration in a heterogeneous Mediterranean ecosystem on Sardinia, Italy, *Water Resour. Res.*, *42*, W08419, doi:10.1029/2005WR004693.
Eva, H. D., A. Brink, and D. Simonetti (2006). Monitoring land cover dynamics in sub-Saharan Africa. Inst. Environ. Sustain. Tech Rep EUR 22498.
Falge, E., et al. (2001), Gap filling strategies for defensible annual sums of net ecosystem exchange, *Agric. For. Meteorol.*, *107*, 43–69.
Food and Agriculture Organization (2011), State of the world's forests 2011. Food and Agriculture Organization of the United Nations, Rome.
Faure, P., and B. Volkoff (1998), Some factors affecting regional differentiation of the soils in the Republic of Benin (West Africa), *CATENA*, *32*, 281–306.
Feddes, R. A., H. Hoff, M. Bruen, T. Dawson, P. De Rosnay, P. Dirmeyer, R. B. Jackson, P. Kabat, A. Kleidon, and A. Lilly (2001), Modeling root water uptake in hydrological and climate models, *Bull. Am. Meteorol. Soc.*, *82*, 2797–2810.
Foken, T., M. Aubinet, J. J. Finnigan, M. Y. Leclerc, M. Mauder, and K. T. Paw U (2011), Results of a panel discussion about the energy balance closure correction for trace gases, *Bull. Am. Meteorol. Soc.*, *92*, ES13–ES18, doi:10.1175/2011BAMS3130.1.
Gash, J. H. C., P. Kabat, B. A. Monteny, M. Amadou, P. Bessemoulin, H. Billing, E. M. Blyth, H. A. R. DeBruin, J. A. Elbers, and T. Friborg (1997), The variability of evaporation during the HAPEX-Sahel intensive observation period, *J. Hydrol.*, *188*, 385–399.
Gee, G. W., and C. A. Federer (1972), Stomatal resistance during senescence of hardwood leaves, *Water Resour. Res.*, *8*, 1456–1460, doi:10.1029/WR008i006p01456.
Giertz, S., and B. Diekkrüger (2003), Analysis of the hydrological processes in a small headwater catchment in Benin (West Africa), *Phys. Chem. Earth Part A.*, *28*, 1333–1341, doi:10.1016/j.pce.2003.09.009.
Gounou, A., F. Guichard, and F. Couvreux (2012), Observations of diurnal cycles over a West African meridional transect: Pre-monsoon and full-monsoon seasons, *Boundary Layer Meteorol.*, *144*, 329–357, doi:10.1007/s10546-012-9723-8.
Granier, A., R. Huc, and S. T. Barigah (1996), Transpiration of natural rain forest and its dependence on climatic factors, *Agric. For. Meteorol.*, *78*, 19–29.
Guengant, J.-P., and Y. Kamara (2012), How can we capitalize on the demographic dividend? Demographics at the heart of development pathways. Savoir Collect.
Guyot, A., J.-M. Cohard, S. Anquetin, S. Galle, and C. R. Lloyd (2009), Combined analysis of energy and water balances to estimate latent heat flux of a sudanian small catchment, *J. Hydrol.*, *375*, 227–240, doi:10.1016/j.jhydrol.2008.12.027.
Guyot, A., J.-M. Cohard, S. Anquetin, and S. Galle (2012), Long-term observations of turbulent fluxes over heterogeneous vegetation using scintillometry and additional observations: A contribution to AMMA under Sudano-Sahelian climate, *Agric. For. Meteorol.*, *154–155*, 84–98, doi:10.1016/j.agrformet.2011.10.008.
Hector, B., L. Séguis, J. Hinderer, J.-M. Cohard, M. Wubda, M. Descloitres, N. Benarrosh, and J.-P. Boy (2015), Water storage changes as a marker for base flow generation processes in a tropical humid basement catchment (Benin): Insights from hybrid gravimetry, *Water Resour. Res.*, *51*, 8331–8361, doi:10.1002/2014WR015773.
Heldmann, M., and M. Doevenspeck (2009), Démographie: Disparités spatiales et taux de croissance élevés: In IMPETUS ATLAS du Benin. Résultats e recherche 2000-2007 (No. 3eme edition). Université de Bonn, Allemagne, Département de Géographie.
Hollinger, D. Y., and A. D. Richardson (2005), Uncertainty in eddy covariance measurements and its application to physiological models, *Tree Physiol.*, *25*, 873.
Houéto, G., B. Fandohan, A. Ouédraogo, E. E. Ago, V. K. Salako, A. E. Assogbadjo, R. G. Kakaï, and B. Sinsin (2012), Floristic and dendrometric analysis of woodlands in the Sudano-Guinean zone: A case study of Belléfoungou forest reserve in Benin, *Acta Bot. Gallica*, *159*, 387–394, doi:10.1080/12538078.2012.735124.
Hsieh, C.-I., G. Katul, and T. Chi (2000), An approximate analytical model for footprint estimation of scalar fluxes in thermally stratified atmospheric flows, *Adv. Water Resour.*, *23*, 765–772.
Jarvis, P. G., and K. G. McNaughton (1986), Stomatal control of transpiration: scaling up from leaf to region, *Adv. Ecol. Res.*, *15*, 49.
Juárez, R. I. N., M. G. Hodnett, R. Fu, M. L. Goulden, and C. von Randow (2007), Control of dry season evapotranspiration over the Amazonian forest as inferred from observations at a southern Amazon Forest site, *J. Clim.*, *20*, 2827–2839, doi:10.1175/JCLI4184.1.
Kelly, C. N., K. J. McGuire, C. F. Miniat, and J. M. Vose (2016), Streamflow response to increasing precipitation extremes altered by forest management, *Geophys. Res. Lett.*, *43*, 3727–3736, doi:10.1002/2016GL068058.
Koster, R. D., et al. (2004), Regions of strong coupling between soil moisture and precipitation, *Science*, *305*, 1138–1140, doi:10.1126/science.1100217.
Kounouhéwa, B., O. Mamadou, G. Koto N'Gobi, and C. N. Awanou (2013), Dynamics and diurnal variations of surface radiation budget over agricultural crops located in Sudanian climate, *Atmos. Clim. Sci.*, *3*, 121–131, doi:10.4236/acs.2013.31014.
Krishnaswamy, J., M. Bonell, B. Venkatesh, B. K. Purandara, S. Lele, M. C. Kiran, V. Reddy, S. Badiger, and K. N. Rakesh (2012), The rain–runoff response of tropical humid forest ecosystems to use and reforestation in the Western Ghats of India, *J. Hydrol.*, *472–473*, 216–237, doi:10.1016/j.jhydrol.2012.09.016.
Lebel, T., et al. (2009), AMMA-CATCH studies in the Sahelian region of West-Africa: An overview, *J. Hydrol.*, *375*, 3–13.
Lelay, M., and S. Galle (2005), How changing rainfall regimes may affect the water balance: a modelling approach in West Africa, *Reg. Hydrol. Impacts Clim. Change Hydroclimatic Var.*, *2*, 203.
Lohou, F., F. Saïd, M. Lothon, P. Durand, and D. Serça (2010), Impact of boundary-layer processes on near-surface turbulence within the West African monsoon, *Boundary Layer Meteorol.*, *136*, 1–23, doi:10.1007/s10546-010-9493-0.
Lothon, M., F. Saïd, F. Lohou, and B. Campistron (2008), Observation of the diurnal cycle in the low troposphere of West Africa, *Mon. Weather Rev.*, *136*, 3477–3500, doi:10.1175/2008MWR2427.1.

Mamadou, O. (2014), Etude des flux d'Evapotranspiration en climat soudanien: comportement comparé de deux couverts végétaux au Bénin. Université de Grenoble (France) et Université d'Abomey-Calavi (Bénin), Abomey-Calavi.
Mamadou, O., J. M. Cohard, S. Galle, C. N. Awanou, A. Diedhiou, B. Kounouhewa, and C. Peugeot (2014), Energy fluxes and surface characteristics over a cultivated area in Benin: Daily and seasonal dynamics, *Hydrol. Earth Syst. Sci.*, *18*, 893–914, doi:10.5194/hess-18-893-2014.
Marticorena, B., B. Chatenet, J. L. Rajot, S. Traoré, M. Coulibaly, A. Diallo, I. Koné, A. Maman, T. NDiaye, and A. Zakou (2010), Temporal variability of mineral dust concentrations over West Africa: Analyses of a pluriannual monitoring from the AMMA Sahelian Dust Transect, *Atmos. Chem. Phys.*, *10*, 8899–8915, doi:10.5194/acp-10-8899-2010.
Mauder, M., and T. Foken (2004), Documentation and instruction manual of the eddy covariance software package TK2. Univ., Abt. Mikrometeorologie Bayreuth.
Maxwell, R. M., J. K. Lundquist, J. D. Mirocha, S. G. Smith, C. S. Woodward, and A. F. B. Tompson (2010), Development of a coupled groundwater–atmosphere model, *Mon. Weather Rev.*, *139*, 96–116, doi:10.1175/2010MWR3392.1.
Miralles, D. G., R. A. M. De Jeu, J. H. Gash, T. R. H. Holmes, and A. J. Dolman (2011), Magnitude and variability of land evaporation and its components at the global scale, *Hydrol. Earth Syst. Sci.*, *15*, 967–981, doi:10.5194/hess-15-967-2011.
Moore, G. W., D. A. Barre, and M. K. Owens (2012), Does shrub removal increase groundwater recharge in southwestern Texas semiarid rangelands?, *Rangel. Ecol. Manag.*, *65*, 1–10, doi:10.2111/REM-D-11-00055.1.
Nepstad, D. C., C. R. de Carvalho, E. A. Davidson, P. H. Jipp, P. A. Lefebvre, G. H. Negreiros, E. D. da Silva, T. A. Stone, S. E. Trumbore, and S. Vieira (1994), The role of deep roots in the hydrological and carbon cycles of Amazonian forests and pastures, *Nature*, *372*, 666–669, doi:10.1038/372666a0.
Novick, K. A., R. Oren, P. C. Stoy, M. B. S. Siqueira, and G. G. Katul (2009), Nocturnal evapotranspiration in eddy-covariance records from three co-located ecosystems in the Southeastern U.S.: Implications for annual fluxes, *Agric. For. Meteorol.*, *149*, 1491–1504, doi:10.1016/j.agrformet.2009.04.005.
Numaguti, A. (1993), Dynamics and energy balance of the hadley circulation and the tropical precipitation zones: Significance of the distribution of evaporation, *J. Atmospheric Sci.*, *50*, 1874–1887, doi:10.1175/1520-0469(1993)050<1874:DAEBOT>2.0.CO;2.
Ouedraogo, I., M. Tigabu, P. Savadogo, H. Compaoré, P. C. Odén, and J. M. Ouadba (2010), Land cover change and its relation with population dynamics in Burkina Faso, *West Africa. Land Degrad. Dev.*, *21*, 453–462, doi:10.1002/ldr.981.
Peña-Arancibia, J. L., A. I. J. M. van Dijk, J. P. Guerschman, M. Mulligan, L. A. (. S.). Bruijnzeel, and T. R. McVicar (2012), Detecting changes in streamflow after partial woodland clearing in two large catchments in the seasonal tropics, *J. Hydrol.*, *416–417*, 60–71, doi:10.1016/j.jhydrol.2011.11.036.
Peugeot, C., et al. (2011), Mesoscale water cycle within the West African Monsoon, *Atmospheric Sci. Lett.*, *12*, 45–50, doi:10.1002/asl.309.
Pielke, R. A., G. Marland, R. A. Betts, T. N. Chase, J. L. Eastman, J. O. Niles, D. d. S. Niyogi, and S. W. Running (2002), The influence of land-use change and landscape dynamics on the climate system: relevance to climate-change policy beyond the radiative effect of greenhouse gases, *Philos. Trans. R. Soc. Lond. Math. Phys. Eng. Sci.*, *360*, 1705–1719, doi:10.1098/rsta.2002.1027.
Quansah, E., M. Mauder, A. A. Balogun, L. K. Amekudzi, L. Hingerl, J. Bliefernicht, and H. Kunstmann (2015), Carbon dioxide fluxes from contrasting ecosystems in the Sudanian Savanna in West Africa, *Carbon Bal. Manag.*, *10*, 1, doi:10.1186/s13021-014-0011-4.
Ramier, D., N. Boulain, B. Cappelaere, F. Timouk, M. Rabanit, C. R. Lloyd, S. Boubkraoui, F. Métayer, L. Descroix, and V. Wawrzyniak (2009), Towards an understanding of coupled physical and biological processes in the cultivated Sahel-1. Energy and water, *J. Hydrol.*, *375*, 204–216.
Richard, A., S. Galle, M. Descloitres, J.-M. Cohard, J.-P. Vandervaere, L. Séguis, and C. Peugeot (2013), Interplay of Riparian Forest and Groundwater in the Hillslope Hydrology of Sudanian West Africa (Northern Benin), *Hydrol. Earth Syst. Sci.*, *17*(12), 5079–96, doi:10.5194/hess-17-5079-2013.
Richardson, A. D., et al. (2006), A multi-site analysis of random error in tower-based measurements of carbon and energy fluxes, *Agric. For. Meteorol.*, *136*, 1–18, doi:10.1016/j.agrformet.2006.01.007.
Seghieri, J., et al. (2009), Relationships between climate, soil moisture and phenology of the woody cover in two sites located along the West African latitudinal gradient, *J. Hydrol.*, *375*, 78–89, doi:10.1016/j.jhydrol.2009.01.023.
Seghieri, J., A. Fournier, F. C. Do, and J.-L. Devineau (2012), Phenology of woody species along the climatic gradient in west tropical Africa. INTECH Open Access Publisher.
Séguis, L., et al. (2011), Contrasted land-surface processes along the West African rainfall gradient, *Atmospheric Sci. Lett.*, *12*, 31–37, doi:10.1002/asl.327.
Snyder, K. A. (2003), Night-time conductance in C3 and C4 species: Do plants lose water at night?, *J. Exp. Bot.*, *54*, 861–865, doi:10.1093/jxb/erg082.
Sultan, B., and S. Janicot (2003), The West African monsoon dynamics. Part II: The "preonset" and "onset" of the summer monsoon, *J. Clim.*, *16*, 3407–3427.
Taylor, C. M., R. A. M. de Jeu, F. Guichard, P. P. Harris, and W. A. Dorigo (2012), Afternoon rain more likely over drier soils, *Nature*, *489*, 423–426, doi:10.1038/nature11377.
Timouk, F., L. Kergoat, E. Mougin, C. R. Lloyd, E. Ceschia, J. M. Cohard, P. Rosnay, P. Hiernaux, V. Demarez, and C. M. Taylor (2009), Response of surface energy balance to water regime and vegetation development in a Sahelian landscape, *J. Hydrol.*, *375*, 178–189.
UN (2015), United Nations, Department of Economic and Social Affairs, Population Division, World Population Prospects: The 2015 Revision, Key Findings and Advance Tables (No. Working Paper N0. ESA/P/WP.241).
Velluet, C., et al. (2014), Building a field- and model-based climatology of local water and energy cycles in the cultivated Sahel annual budgets and seasonality, *Hydrol. Earth Syst. Sci.*, *18*, 5001–5024, doi:10.5194/hess-18-5001-2014.
Vouillamoz, J. M., F. M. A. Lawson, N. Yalo, and M. Descloitres (2015), Groundwater in hard rocks of Benin: Regional storage and buffer capacity in the face of change, *J. Hydrol.*, *520*, 379–386, doi:10.1016/j.jhydrol.2014.11.024.
Vourlitis, G. L., N. P. Filho, M. M. S. Hayashi, J. de Souza Nogueira, F. T. Caseiro, and J. H. Campelo (2002), Seasonal variations in the evapotranspiration of a transitional tropical forest of Mato Grosso, Brazil, *Water Resour. Res.*, *38*(6), 30-1–30-11, doi:10.1029/2000WR000122.
Vourlitis, G. L., J. de Souza Nogueira, F. de Almeida Lobo, and O. B. Pinto (2015), Variations in evapotranspiration and climate for an Amazonian semi-deciduous forest over seasonal, annual, and El Niño cycles, *Int. J. Biometeorol.*, *59*, 217–230, doi:10.1007/s00484-014-0837-1.
Wang, G., and E. A. Eltahir (2000), Biosphere-atmosphere interactions over West Africa. I: Development and validation of a coupled dynamic model, *Q. J. R. Meteorol. Soc.*, *126*, 1239–1260.
Weaver, C. P., and R. Avissar (2001), Atmospheric disturbances caused by human modification of the landscape, *Bull. Am. Meteorol. Soc.*, *82*, 269–281, doi:10.1175/1520-0477(2001)082<0269:ADCBHM>2.3.CO;2.
Weiss, M., F. Baret, G. J. Smith, I. Jonckheere, and P. Coppin (2004), Review of methods for in situ leaf area index (LAI) determination, *Agric. For. Meteorol.*, *121*, 37–53, doi:10.1016/j.agrformet.2003.08.001.
White, F. (1983), The vegetation of Africa: A descriptive memoir to accompany the UNESCO/AETFAT/UNSO vegetation map of Africa, *Geogr. J.*, *151*, 132, doi:10.2307/633318.

Wilson, K., et al. (2002), Energy balance closure at FLUXNET sites, *Agric. For. Meteorol.*, *113*, 223–243.
Xue, Y., H.-M. H. Juang, W.-P. Li, S. Prince, R. DeFries, Y. Jiao, and R. Vasic (2004), Role of land surface processes in monsoon development: East Asia and West Africa, *J. Geophys. Res.*, *109*, D03105, doi:10.1029/2003JD003556.
Zhang, M., X. Wei, P. Sun, and S. Liu (2012), The effect of forest harvesting and climatic variability on runoff in a large watershed: The case study in the Upper Minjiang River of Yangtze River basin, *J. Hydrol.*, *464–465*, 1–11, doi:10.1016/j.jhydrol.2012.05.050.